

Yanyang Lu; Bo Shen

Mobile robot localization under stochastic communication protocol

*Kybernetika*, Vol. 56 (2020), No. 1, 152–169

Persistent URL: <http://dml.cz/dmlcz/148101>

## Terms of use:

© Institute of Information Theory and Automation AS CR, 2020

Institute of Mathematics of the Czech Academy of Sciences provides access to digitized documents strictly for personal use. Each copy of any part of this document must contain these *Terms of use*.



This document has been digitized, optimized for electronic delivery and stamped with digital signature within the project *DML-CZ: The Czech Digital Mathematics Library* <http://dml.cz>

# MOBILE ROBOT LOCALIZATION UNDER STOCHASTIC COMMUNICATION PROTOCOL

YANYANG LU AND BO SHEN

In this paper, the mobile robot localization problem is investigated under the stochastic communication protocol (SCP). In the mobile robot localization system, the measurement data including the distance and the azimuth are received by multiple sensors equipped on the robot. In order to relieve the network burden caused by network congestion, the SCP is introduced to schedule the transmission of the measurement data received by multiple sensors. The aim of this paper is to find a solution to the robot localization problem by designing a time-varying filter for the mobile robot such that the filtering error dynamics satisfies the  $H_\infty$  performance requirement over a finite horizon. First, a Markov chain is introduced to model the transmission of measurement data. Then, by utilizing the stochastic analysis technique and completing square approach, the gain matrices of the desired filter are designed in term of a solution to two coupled backward recursive Riccati equations. Finally, the effectiveness of the proposed filter design scheme is shown in an experimental platform.

*Keywords:* localization, mobile robot, Riccati equations, stochastic communication protocol

*Classification:* 93E11, 93C95

## 1. INTRODUCTION

Over the past decades, the mobile robot has a wide range of applications in various areas such as industry, intelligent transportation, military, space exploration, and so on. As a fundamental issue in robot field, the localization problem has received a great deal of research attention and a great number of results have been reported in the literature, see e. g. [1, 13, 18, 21, 24, 25, 33, 35]. For example, in [35], a novel robust extended  $H_\infty$  filtering approach has been proposed to deal with the mobile robot localization problem. In [33], a new  $H_\infty$  filter has been designed for discrete time-varying systems with missing measurements and quantization effects and the filtering scheme proposed has been successfully applied to the mobile robot localization problem. In [13], an extended Kalman filtering algorithm has been proposed to solve the mobile robot localization problem where a Doppler-azimuth radar is used to measure the Doppler-shift and azimuth measurements.

In reality, when the robot moves, some obstacles may appear between the sensor and the landmark. Therefore, the measurement data received by the sensor from the landmark might be inaccurate at some time instants, which makes the localization inaccurate. In order to reduce the inaccuracy of localization brought by the obstacle, a multiple sensor strategy has been applied in the mobile robot localization problem, see e.g. [2, 16, 17, 22, 23, 36]. However, the transmission of the measurement data will increase the burden of communication network as the number of sensors increases. In order to ease the network burden or avoid the network congestion, the communication protocols have been often adopted in the networked systems such as weighted try-once-discard protocol [39], round-robin protocol [6, 26], event-triggered protocol [11, 15, 20, 29], stochastic communication protocol (SCP) [9, 38], and so on.

The SCP whose main idea is that only one sensor is allowed to access to the network for signal transmission at a certain time instant, has gradually become a hot research topic in networked systems [5, 9, 19, 31, 32, 38]. For the purpose of effectively coping with the phenomena of data congestion/collision, the SCP has been introduced in [5] and the neural network based output-feedback control problem under SCP has been investigated for a class of nonlinear systems. In [19], the observer-based stabilization problem has been investigated for a class of discrete-time nonlinear stochastic networked systems under SCP. In [31], the finite-horizon  $H_\infty$  state estimation problem has been studied for a class of discrete time-varying genetic regulatory networks with quantization effects under SCP. Nevertheless, the mobile robot localization problem under SCP has not yet gained adequate attention.

Motivated by the aforementioned discussions, in this paper, we aim to investigate the mobile robot localization problem under SCP. Our focus is on the design of an  $H_\infty$  filter to ensure that the filtering error satisfies the  $H_\infty$  performance requirement over a given finite horizon. The main challenges we encounter are listed as follows: 1) *how to formulate a mathematical model accounting for the SCP and 2) how to design the filter and the corresponding filter based mobile robot localization algorithm?* We shall overcome the difficulties identified above by finding a solution to the so-called mobile robot localization problem under SCP.

The main contributions of this paper can be summarized as follows:

- 1) the SCP is, for the first time, considered in mobile robot localization problem;
- 2) two coupled backward recursive Riccati difference equations are obtained to design the filter gain matrices; and
- 3) based on the proposed filter design scheme, the localization algorithm of the mobile robot is given.

Finally, the effectiveness of the proposed localization algorithm is verified in an experimental platform.

The remainder of this paper is organized as follows. In Section 2, the mobile robot kinematic model, the measurement model and the SCP are described. In Section 3, the desired filter is designed and the localization algorithm is given. In Section 4, a simulation experiment is implemented. Some conclusions are provided in Section 5.

**Notation.** The notation used here is fairly standard except where otherwise stated.  $\mathbb{R}^n$  and  $\mathbb{R}^{n \times m}$  denote, respectively, the  $n$  dimensional Euclidean space and the set of all  $n \times m$  real matrices. The notation  $X \geq Y$  ( $X > Y$ ), where  $X$  and  $Y$  are real symmetric matrices, means that  $X - Y$  is positive semi-definite (positive definite).  $\text{Prob}\{\cdot\}$  means the occurrence probability of the event “ $\cdot$ ”.  $\mathbb{E}\{x\}$  denotes the expectation of the stochastic variable  $x$ .  $I$  represents the identity matrix of compatible dimensions.  $\text{diag}\{\dots\}$  stands for a block-diagonal matrix.  $\|x\|$  refers to the Euclidean norm of a vector  $x$ .  $M^T$  and  $M^\dagger \in \mathbb{R}^{n \times m}$  represent the transpose and the Moore-Penrose pseudo inverse of matrix  $M \in \mathbb{R}^{m \times n}$ .

## 2. PROBLEM FORMULATION

### 2.1. Mobile robot kinematic model

Consider a two-wheeled mobile robot which is shown in Figure 1.

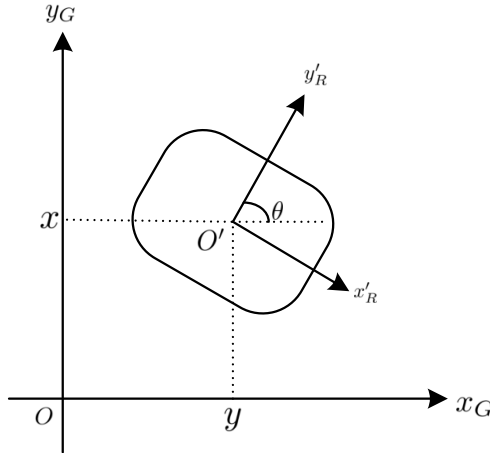


**Fig. 1.** Mobile robot model.

The mobile robot kinematic model is described as follows [33, 35]:

$$\begin{cases} \dot{x}(t) = v(t) \cos \theta(t) \\ \dot{y}(t) = v(t) \sin \theta(t) \\ \dot{\theta}(t) = \bar{\omega}(t) \end{cases} \quad (1)$$

where  $(x(t), y(t))$  is the position of mobile robot,  $\theta(t)$  is the angle between the  $x_G$  axis and the mobile robot forward axis  $y'_R$ ,  $v(t)$  is the displacement of the mobile robot and  $\bar{\omega}(t)$  is the angular velocity of the mobile robot. The displacement and angular velocity of the robot are usually obtained by the odometer and they are assumed to be constant over the sampling period. Then, the continuous-time system (1) is discretized to the

following system:

$$\begin{cases} x(k+1) = x(k) + \Delta T v(k) \cos \theta(k) \\ y(k+1) = y(k) + \Delta T v(k) \sin \theta(k) \\ \theta(k+1) = \theta(k) + \Delta T \bar{\omega}(k) \end{cases} \quad (2)$$

where  $\Delta T$  is the sampling period.

By setting  $X(k) = [x^T(k) \ y^T(k) \ \theta^T(k)]^T$  and  $u(k) = \begin{bmatrix} \Delta T v(k) \\ \Delta T \bar{\omega}(k) \end{bmatrix} := \begin{bmatrix} u_1(k) \\ u_2(k) \end{bmatrix}$ , the system (2) can be rewritten as

$$X(k+1) = f(X(k), u(k)) \quad (3)$$

where

$$f(X(k), u(k)) = X(k) + \begin{bmatrix} u_1(k) \cos \theta(k) \\ u_1(k) \sin \theta(k) \\ u_2(k) \end{bmatrix}.$$

By expanding the nonlinear function  $f(X(k), u(k))$  in a Taylor series about the estimate  $\hat{X}(k)$ , (3) can be further expressed by

$$X(k+1) = A(k)X(k) + \phi(k) \quad (4)$$

where

$$\begin{aligned} A(k) &= \begin{bmatrix} \frac{\partial f_x}{\partial x(k)} & \frac{\partial f_x}{\partial y(k)} & \frac{\partial f_x}{\partial \theta(k)} \\ \frac{\partial f_y}{\partial x(k)} & \frac{\partial f_y}{\partial y(k)} & \frac{\partial f_y}{\partial \theta(k)} \\ \frac{\partial f_\theta}{\partial x(k)} & \frac{\partial f_\theta}{\partial y(k)} & \frac{\partial f_\theta}{\partial \theta(k)} \end{bmatrix} \Bigg|_{X(k)=\hat{X}(k)} \\ &= \begin{bmatrix} 1 & 0 & -u_1(k) \sin \hat{\theta}(k) \\ 0 & 1 & u_1(k) \cos \hat{\theta}(k) \\ 0 & 0 & 1 \end{bmatrix} \end{aligned}$$

and  $\phi(k) = f(\hat{X}(k), u(k)) - A(k)\hat{X}(k) + \varrho_{X(k)}$ . Here,  $\varrho_{X(k)}$  represents the higher order terms occurring in the Taylor expansions of the nonlinear function  $f(X(k), u(k))$ .

**Remark 2.1.** It is well recognized that the evolution of the system (4) depends primarily on the system matrix  $A(k)$  and the nonlinear term  $\phi(k)$  (also known as linearization error) plays a relatively less important role. As such, a conventional way is to treat the nonlinear term  $\phi(k)$  as one of the sources for disturbances. On the other hand, it is inevitable that the system states are contaminated by external noises. For mathematical convenience, we slightly abuse the notation  $\phi(k)$  to include both the linearization errors and the externally environmental noises. Moreover,  $\phi(k)$  is assumed to belong to  $l_2[0, N-1]$ .

## 2.2. Measurement model

The points  $M_i$  ( $i = 1, 2, 3 \dots L$ ) are chosen as landmarks. Denote the measurement vector of the  $i$ th sensor at the time instant  $k$  by  $\tilde{z}_i(k) = [d_i^T(k) \ \varphi_i^T(k)]^T$ . As shown in

Figure 2, the distance  $d_i(k)$  from mobile robot position  $(x(k), y(k))$  to the  $i$ th landmark  $M_i(x_{M_i}, y_{M_i})$  can be expressed by

$$d_i(k) = \sqrt{(x_{M_i} - x(k))^2 + (y_{M_i} - y(k))^2}. \quad (5)$$

The azimuth  $\varphi_i(k)$  at time instant  $k$  can be expressed by

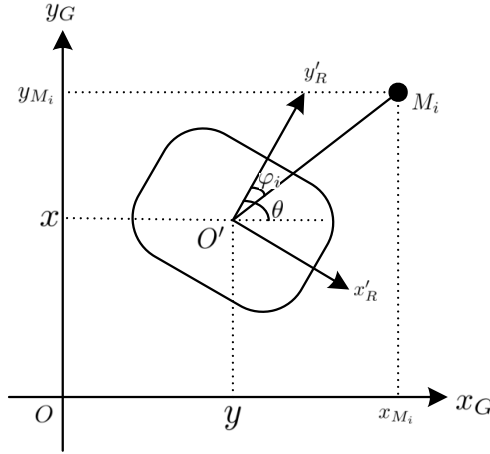


Fig. 2. Absolute measurements.

$$\varphi_i(k) = \theta(k) - \arctan\left(\frac{y_{M_i} - y(k)}{x_{M_i} - x(k)}\right). \quad (6)$$

Consequently, from (5) and (6), the measurement model can be obtained as follows

$$\tilde{z}_i(k) = g_i(X(k)) = \begin{bmatrix} \sqrt{(x_{M_i} - x(k))^2 + (y_{M_i} - y(k))^2} \\ \theta(k) - \arctan\left(\frac{y_{M_i} - y(k)}{x_{M_i} - x(k)}\right) \end{bmatrix}. \quad (7)$$

Again, using Taylor series expansions, the measurement model (7) can be rewritten as

$$\tilde{z}_i(k) = C_i(k)X(k) + v_i(k) \quad (8)$$

where

$$C_i(k) = \begin{bmatrix} \frac{\partial g_{d_i(k)}}{\partial x(k)} & \frac{\partial g_{d_i(k)}}{\partial y(k)} & \frac{\partial g_{d_i(k)}}{\partial \theta(k)} \\ \frac{\partial g_{\varphi_i(k)}}{\partial x(k)} & \frac{\partial g_{\varphi_i(k)}}{\partial y(k)} & \frac{\partial g_{\varphi_i(k)}}{\partial \theta(k)} \end{bmatrix} \Bigg|_{X(k)=\hat{X}(k)} = \begin{bmatrix} \frac{-(x_{M_i} - \hat{x}(k))}{\sqrt{(x_{M_i} - \hat{x}(k))^2 + (y_{M_i} - \hat{y}(k))^2}} & \frac{-(y_{M_i} - \hat{y}(k))}{\sqrt{(x_{M_i} - \hat{x}(k))^2 + (y_{M_i} - \hat{y}(k))^2}} & 0 \\ \frac{-(y_{M_i} - \hat{y}(k))}{(x_{M_i} - \hat{x}(k))^2 + (y_{M_i} - \hat{y}(k))^2} & \frac{x_{M_i} - \hat{x}(k)}{(x_{M_i} - \hat{x}(k))^2 + (y_{M_i} - \hat{y}(k))^2} & 1 \end{bmatrix}$$

and  $v_i(k)$  represents linearization errors and the measurement noises which is also assumed to belong to  $l_2[0, N - 1]$ .

Denote

$$\begin{aligned}\tilde{z}(k) &= [ \tilde{z}_1^T(k) \quad \tilde{z}_2^T(k) \quad \cdots \quad \tilde{z}_L^T(k) ]^T \in \mathbb{R}^{2L}, \\ C(k) &= [ C_1^T(k) \quad C_2^T(k) \quad \cdots \quad C_L^T(k) ]^T \in \mathbb{R}^{2L \times 3}, \\ v(k) &= [ v_1^T(k) \quad v_2^T(k) \quad \cdots \quad v_L^T(k) ]^T \in \mathbb{R}^{2L}.\end{aligned}$$

Then, the measurement output  $\tilde{z}(k)$  can be described by the following compact expression

$$\tilde{z}(k) = C(k)X(k) + v(k). \quad (9)$$

### 2.3. Stochastic communication protocol

At each communication time instant, only one sensor has the privilege to transmit its measurement data to the remote filters for the purpose of easing the communication network burden. To this end, the SCP is introduced to manage which sensor acquires the privilege to send its measurement data. Denote by  $\ell(k)$  the selected sensor at time instant  $k$  and we regard  $\ell(k) \in \{1, 2, 3 \dots L\}$  as a random process described by a Markov chain with the transition probability matrix  $\Xi(k) = [\pi_{qr}(k)]_{L \times L}$  defined as follows

$$\pi_{qr}(k) = \text{Prob}\{\ell(k+1) = r | \ell(k) = q\}, \quad \forall q, r \in \{1, 2, 3 \dots L\}, \quad (10)$$

where  $\pi_{qr}(k) \geq 0$  ( $q, r \in \{1, 2, 3 \dots L\}$ ) means the transition probability from  $q$  to  $r$  at time instant  $k$  and  $\sum_{r=1}^L \pi_{qr}(k) = 1$ .

The measurement signal after the transmission via the network is described as follows

$$z(k) \triangleq [ z_1^T(k) \quad z_2^T(k) \quad \cdots \quad z_L^T(k) ]^T \in \mathbb{R}^{2L}. \quad (11)$$

The updating rule for  $z_q(k)$  ( $q = 1, 2, 3 \dots L$ ) under the SCP is expressed by

$$z_q(k) = \begin{cases} \tilde{z}_q(k) + \varphi_q(k), & q = \ell(k), \\ z_q(k-1), & \text{otherwise,} \end{cases} \quad (12)$$

where  $\varphi_q(k)$  is the exogenous disturbance which is also assumed to belong to  $l_2[0, N - 1]$ .

Defining

$$\begin{aligned}\Psi_{\ell(k)} &\triangleq \text{diag}\{\delta(\ell(k) - 1)I_{2 \times 2}, \delta(\ell(k) - 2)I_{2 \times 2}, \dots, \delta(\ell(k) - L)I_{2 \times 2}\} \in \mathbb{R}^{2L \times 2L}, \\ \varphi(k) &\triangleq [ \varphi_1^T(k) \quad \varphi_2^T(k) \quad \cdots \quad \varphi_L^T(k) ]^T \in \mathbb{R}^{2L},\end{aligned}$$

where  $\delta(\cdot)$  stands for the Kronecker delta function taking values on 0 or 1, we obtain the actually received measurements by the filter as follows

$$z(k) = \Psi_{\ell(k)}(\tilde{z}(k) + \varphi(k)) + (I - \Psi_{\ell(k)})z(k-1). \quad (13)$$

Let

$$\begin{aligned} \mathcal{X}(k) &\triangleq [ X^T(k) \quad z^T(k-1) ]^T \in \mathbb{R}^{2L+3}, \\ w(k) &\triangleq [ \phi^T(k) \quad v^T(k) \quad \varphi^T(k) ]^T \in \mathbb{R}^{4L+3}. \end{aligned}$$

For each possible  $\ell(k) = q \in \{1, 2, 3 \dots L\}$ , it is obtained from (4), (9) and (13) that

$$\begin{cases} \mathcal{X}(k+1) = \mathcal{A}_q(k)\mathcal{X}(k) + \mathcal{B}_q(k)w(k) \\ z(k) = \mathcal{C}_q(k)\mathcal{X}(k) + \mathcal{D}_q(k)w(k) \end{cases} \quad (14)$$

where

$$\begin{aligned} \mathcal{A}_q(k) &= \begin{bmatrix} A(k) & 0 \\ \Psi_q C(k) & I - \Psi_q \end{bmatrix}, \quad \mathcal{B}_q(k) = \begin{bmatrix} I & 0 & 0 \\ 0 & \Psi_q & \Psi_q \end{bmatrix}, \\ \mathcal{C}_q(k) &= [ \Psi_q C(k) \quad I - \Psi_q ], \quad \mathcal{D}_q(k) = [ 0 \quad \Psi_q \quad \Psi_q ]. \end{aligned}$$

We construct a filter for the augmented system (14) as follows

$$\hat{\mathcal{X}}(k+1) = \mathcal{A}_q(k)\hat{\mathcal{X}}(k) + K_q(k)(z(k) - \mathcal{C}_q(k)\hat{\mathcal{X}}(k)) \quad (15)$$

where  $\hat{\mathcal{X}}(k)$  represents the estimate of the state  $\mathcal{X}(k)$  and  $K_q(k)$  is the gain matrix to be designed.

By denoting  $e(k) = \mathcal{X}(k) - \hat{\mathcal{X}}(k)$ , the following filtering error dynamics is obtained

$$e(k+1) = (\mathcal{A}_q(k) - K_q(k)\mathcal{C}_q(k))e(k) + (\mathcal{B}_q(k) - K_q(k)\mathcal{D}_q(k))w(k). \quad (16)$$

In this paper, our objective is to design a filter of structure (15) such that the error dynamic system (16) satisfies the following performance requirement

$$\mathbb{E} \left\{ \sum_{k=0}^{N-1} (\|e(k)\|^2 - \gamma^2 \|w(k)\|^2) \right\} - \gamma^2 e^T(0)\mathcal{S}e(0) < 0 \quad (17)$$

where  $\gamma > 0$  is the disturbance attenuation level and  $\mathcal{S} > 0$  is the given matrix.

### 3. MAIN RESULTS

In derivation of our main results, the following lemmas will be used.

**Lemma 3.1.** Let matrices  $G$ ,  $M$  and  $\Gamma$  be given with appropriate dimensions. The following matrix equation

$$GXM = \Gamma \quad (18)$$

has a solution  $X$  if and only if  $GG^\dagger\Gamma M^\dagger M = \Gamma$ . Moreover, if the condition is met, the solution to (18) can be represented by

$$X = G^\dagger\Gamma M^\dagger + Y - G^\dagger G Y M M^\dagger$$

where  $Y$  is a matrix with appropriate dimensions.



**Lemma 3.2.** Consider the system (4) under the SCP and let the filter gain matrix  $\{K_q(k)\}_{0 \leq k \leq N-1}$  ( $q \in \{1, 2, 3 \dots L\}$ ), the disturbance attenuation level  $\gamma > 0$  and the matrix  $\mathcal{S} > 0$  be given. For any disturbance sequences  $\{w(k)\}_{0 \leq k \leq N-1}$ , the error dynamic system (16) satisfies the  $H_\infty$  performance requirement (17) if there exists a family of positive definite matrices  $\{P_q(k)\}_{0 \leq k \leq N-1}$  (with final condition  $P_q(N) = 0, q \in \{1, 2, 3 \dots L\}$ ) satisfying the following backward discrete Riccati difference equation

$$\begin{aligned} P_q(k) = & (\mathcal{A}_q(k) - K_q(k)\mathcal{C}_q(k))^T \bar{P}_q(k+1) (\mathcal{A}_q(k) - K_q(k)\mathcal{C}_q(k)) + I \\ & + (\mathcal{A}_q(k) - K_q(k)\mathcal{C}_q(k))^T \bar{P}_q(k+1) (\mathcal{B}_q(k) - K_q(k)\mathcal{D}_q(k)) \Delta_q^{-1}(k) \\ & \times (\mathcal{B}_q(k) - K_q(k)\mathcal{D}_q(k))^T \bar{P}_q(k+1) (\mathcal{A}_q(k) - K_q(k)\mathcal{C}_q(k)) \end{aligned} \quad (19)$$

with

$$\begin{cases} \Delta_q(k) = \gamma^2 I - (\mathcal{B}_q(k) - K_q(k)\mathcal{D}_q(k))^T \bar{P}_q(k+1) (\mathcal{B}_q(k) - K_q(k)\mathcal{D}_q(k)) > 0 \\ P_q(0) \leq \gamma^2 \mathcal{S} \end{cases} \quad (20)$$

where

$$\bar{P}_q(k+1) = \sum_{r=1}^L \pi_{qr}(k) P_r(k+1). \quad (21)$$

*Proof.* Consider the following Lyapunov functional candidate for error system (16)

$$V_{\ell(k)}(k) = e^T(k) P_{\ell(k)}(k) e(k). \quad (22)$$

We construct the following equation:

$$\begin{aligned} J_{\ell(k)}(k) = & V_{\ell(k+1)}(k+1) - V_{\ell(k)}(k) + e^T(k) e(k) - \gamma^2 w^T(k) w(k) \\ & - (e^T(k) e(k) - \gamma^2 w^T(k) w(k)). \end{aligned} \quad (23)$$

For  $\ell(k) = q$ , one has

$$\begin{aligned} \mathbb{E}\{J_q(k)\} = & \mathbb{E}\left\{ \left( (\mathcal{A}_q(k) - K_q(k)\mathcal{C}_q(k)) e(k) \right. \right. \\ & + (\mathcal{B}_q(k) - K_q(k)\mathcal{D}_q(k)) w(k) \Big)^T \\ & \times \bar{P}_q(k+1) \left( (\mathcal{A}_q(k) - K_q(k)\mathcal{C}_q(k)) e(k) \right. \\ & + (\mathcal{B}_q(k) - K_q(k)\mathcal{D}_q(k)) w(k) \\ & - e^T(k) P_q(k) e(k) + e^T(k) e(k) \\ & \left. \left. - \gamma^2 w^T(k) w(k) - (e^T(k) e(k) - \gamma^2 w^T(k) w(k)) \right) \right\}. \end{aligned} \quad (24)$$

Applying the completing square technique, we have

$$\mathbb{E}\{J_q(k)\} = \mathbb{E}\left\{ e^T(k) \left( (\mathcal{A}_q(k) - K_q(k)\mathcal{C}_q(k))^T \bar{P}_q(k+1) \right. \right.$$

$$\begin{aligned}
& \times (\mathcal{A}_q(k) - K_q(k)\mathcal{C}_q(k)) - P_q(k) + I)e(k) \\
& + (w^*(k))^T \Delta_q(k) w^*(k) \\
& - (w(k) - w^*(k))^T \Delta_q(k) (w(k) - w^*(k)) \Big\} \\
& - \mathbb{E} \left\{ e^T(k) e(k) - \gamma^2 w^T(k) w(k) \right\} \tag{25}
\end{aligned}$$

where

$$w^*(k) = \Delta_q^{-1}(k) (\mathcal{B}_q(k) - K_q(k)\mathcal{D}_q(k))^T \bar{P}_q(k+1) (\mathcal{A}_q(k) - K_q(k)\mathcal{C}_q(k)) e(k).$$

Taking the sum on both sides of (25) from 0 to  $N-1$  with respect to  $k$ , we obtain

$$\begin{aligned}
& \mathbb{E} \left\{ e^T(N) P_{\ell(N)}(N) e(N) - e^T(0) P_{\ell(0)}(0) e(0) \right\} \\
& = \mathbb{E} \left\{ - \sum_{k=0}^{N-1} (w(k) - w^*(k))^T \Delta_q(k) (w(k) - w^*(k)) \right. \\
& \quad \left. - \sum_{k=0}^{N-1} (e^T(k) e(k) - \gamma^2 w^T(k) w(k)) \right\}. \tag{26}
\end{aligned}$$

Since  $\Delta_q(k) > 0$ ,  $P_q(0) \leq \gamma^2 \mathcal{S}$  and  $P_q(N) = 0$ , we have

$$\begin{aligned}
& \mathbb{E} \left\{ \sum_{k=0}^{N-1} (\|e(k)\|^2 - \gamma^2 \|w(k)\|^2) \right\} - \gamma^2 e^T(0) \mathcal{S} e(0) \\
& = \mathbb{E} \left\{ - \sum_{k=0}^{N-1} (w(k) - w^*(k))^T \Delta_q(k) (w(k) - w^*(k)) \right. \\
& \quad \left. + e^T(0) (P_{\ell(0)}(0) - \gamma^2 \mathcal{S}) e(0) \right\} < 0, \tag{27}
\end{aligned}$$

which means that the  $H_\infty$  performance requirement (17) is satisfied. The proof is complete.  $\square$

So far, we have conducted the  $H_\infty$  performance analysis in terms of the solvability of a backward Riccati equation in Lemma 3.2. In the next stage, we compute the desired filter gain matrix  $K_q(k)$  under the worst situation  $w(k) = w^*(k)$ . For this purpose, we rewrite the error system (16) as follows

$$e(k+1) = \bar{\mathcal{A}}_q(k) e(k) + \Upsilon_q(k), \tag{28}$$

where

$$\begin{aligned}
\bar{\mathcal{A}}_q(k) &= \mathcal{A}_q(k) + (\mathcal{B}_q(k) - K_q(k)\mathcal{D}_q(k)) \Omega_q(k), \\
\Upsilon_q(k) &= -K_q(k)\mathcal{C}_q(k) e(k), \\
\Omega_q(k) &= \Delta_q^{-1}(k) (\mathcal{B}_q(k) - K_q(k)\mathcal{D}_q(k))^T \bar{P}_q(k+1) (\mathcal{A}_q(k) - K_q(k)\mathcal{C}_q(k)) \tag{29}
\end{aligned}$$

and define a cost function as follows

$$\bar{J}_q^*(k) = \mathbb{E} \left\{ \sum_{k=0}^{N-1} (\|e(k)\|^2 + \|\Upsilon_q(k)\|^2) \right\}. \quad (30)$$

**Theorem 3.3.** Consider the system (4) under the SCP constraints. Let the disturbance level  $\gamma > 0$  and the matrix  $\mathcal{S} > 0$  be given. The error system (16) satisfies the  $H_\infty$  performance requirement (17) if there exists a family of positive definite matrices  $(P_q(k), Q_q(k))_{0 \leq k \leq N-1}$  and matrix  $K_q(k)_{0 \leq k \leq N-1}$  ( $q \in \{1, 2, 3 \dots L\}$ ) satisfying the recursive RDE (19) and the following RDE

$$\begin{cases} Q_q(k) = \bar{\mathcal{A}}_q^T(k) \bar{Q}_q(k+1) \bar{\mathcal{A}}_q(k) + I - \bar{\mathcal{A}}_q^T(k) \bar{Q}_q(k+1) \Lambda_q^{-1}(k) \bar{Q}_q(k+1) \bar{\mathcal{A}}_q(k) \\ Q_q(N) = 0 \end{cases} \quad (31)$$

with

$$\begin{cases} P_q(0) \leq \gamma^2 \mathcal{S}, P_q(N) = 0, \\ \Lambda_q(k) = \bar{Q}_q(k+1) + I > 0, \end{cases} \quad (32)$$

where

$$\bar{Q}_q(k+1) = \sum_{r=1}^L \pi_{qr}(k) Q_r(k+1). \quad (33)$$

Moreover, if the above condition is met, the filter gain matrix is given by

$$K_q(k) = \mathcal{N}_q(k) \mathcal{C}_q^\dagger(k) + Y_q(k) - Y_q(k) \mathcal{C}_q(k) \mathcal{C}_q^\dagger(k), \quad (34)$$

where  $\mathcal{N}_q(k) = \Lambda_q^{-1}(k) \bar{Q}_q(k+1) \bar{\mathcal{A}}_q(k)$  and  $Y_q(k)$  is a matrix with appropriate dimensions. Meanwhile, the minimum of the cost function of (30) is given by

$$\bar{J}_q^*(k) = e^T(0) Q_{\ell(0)}(0) e(0) \quad (35)$$

*Proof.* First, it follows from Lemma 3.2 that, if there exists a solution  $P_q(k)$  such that (19) holds with  $\Delta_q(k) > 0$  and  $P_q(0) \leq \gamma^2 \mathcal{S}$ , the system satisfies the  $H_\infty$  performance requirement. In this case, the worst-case disturbance can be expressed as  $w^*(k) = \Omega_q(k) e(k)$ . In what follows, by employing the worst-case disturbance, we aim to provide a design scheme for the gain matrices of the time-varying filter, i. e.,  $K_q(k)_{0 \leq k \leq N-1}$ . For this purpose, we define

$$\mathcal{J}_{\ell(k)}(k) = e^T(k+1) Q_{\ell(k+1)}(k+1) e(k+1) - e^T(k) Q_{\ell(k)}(k) e(k). \quad (36)$$

For  $\ell(k) = q$ , noticing (28) and taking mathematical expectation on both sides of (36), we have

$$\mathbb{E}\{\mathcal{J}_q(k)\} = \mathbb{E} \left\{ (\bar{\mathcal{A}}_q(k) e(k) + \Upsilon_q(k))^T \bar{Q}_q(k+1) (\bar{\mathcal{A}}_q(k) e(k) + \Upsilon_q(k)) \right\}$$

$$\begin{aligned}
& - e^T(k)Q_q(k)e(k) \Big\} \\
= & \mathbb{E} \left\{ e^T(k)(\bar{\mathcal{A}}_q^T(k)\bar{Q}_q(k+1)\bar{\mathcal{A}}_q(k) - Q_q(k))e(k) \right. \\
& \left. + 2e^T(k)\bar{\mathcal{A}}_q^T(k)\bar{Q}_q(k+1)\Upsilon_q(k) + \Upsilon_q^T(k)\bar{Q}_q(k+1)\Upsilon_q(k) \right\}. \quad (37)
\end{aligned}$$

Then, it follows that

$$\begin{aligned}
\mathbb{E}\{\mathcal{J}_q(k)\} = & \mathbb{E} \left\{ e^T(k)(\mathcal{A}_q^T(k)\bar{Q}_q(k+1)\mathcal{A}_q(k) - Q_q(k))e(k) \right. \\
& \left. + 2e^T(k)\bar{\mathcal{A}}_q^T(k)\bar{Q}_q(k+1)\Upsilon_q(k) + \Upsilon_q^T(k)\bar{Q}_q(k+1)\Upsilon_q(k) \right\} \\
& + \mathbb{E} \left\{ \|e(k)\|^2 + \|\Upsilon_q(k)\|^2 - \|e(k)\|^2 - \|\Upsilon_q(k)\|^2 \right\} \\
= & \mathbb{E} \left\{ e^T(k)(\bar{\mathcal{A}}_q^T(k)\bar{Q}_q(k+1)\bar{\mathcal{A}}_q(k) - Q_q(k) + I)e(k) \right. \\
& \left. + 2e^T(k)\bar{\mathcal{A}}_q^T(k)\bar{Q}_q(k+1)\Upsilon_q(k) \right. \\
& \left. + \Upsilon_q^T(k)(\bar{Q}_q(k+1) + I)\Upsilon_q(k) - \|e(k)\|^2 - \|\Upsilon_q(k)\|^2 \right\}. \quad (38)
\end{aligned}$$

Applying the completing square method again, we have

$$\begin{aligned}
\mathbb{E}\{\mathcal{J}_q(k)\} = & \mathbb{E} \left\{ e^T(k) \left( \bar{\mathcal{A}}_q^T(k)\bar{Q}_q(k+1)\bar{\mathcal{A}}_q(k) - Q_q(k) + I \right. \right. \\
& \left. \left. - \bar{\mathcal{A}}_q^T(k)\bar{Q}_q(k+1)\Lambda_q^{-1}(k)\bar{Q}_q(k+1)\bar{\mathcal{A}}_q(k) \right) e(k) \right. \\
& \left. + (\Upsilon_q(k) - \check{\Upsilon}_q(k))^T \Lambda_q(k) (\Upsilon_q(k) - \check{\Upsilon}_q(k)) - \|e(k)\|^2 - \|\Upsilon_q(k)\|^2 \right\}, \quad (39)
\end{aligned}$$

where

$$\check{\Upsilon}_q(k) = -\Lambda_q^{-1}(k)\bar{Q}_q(k+1)\bar{\mathcal{A}}_q(k)e(k). \quad (40)$$

Therefore, it follows from (31) that

$$\begin{aligned}
\bar{J}_q^*(k) = & \mathbb{E} \left\{ \sum_{k=0}^{N-1} (\|e(k)\|^2 + \|\Upsilon_q(k)\|^2) \right\} \\
= & \mathbb{E} \left\{ \sum_{k=0}^{N-1} \left( (\Upsilon_q(k) - \check{\Upsilon}_q(k))^T \Lambda_q(k) (\Upsilon_q(k) - \check{\Upsilon}_q(k)) \right) \right\} + e^T(0)Q_{\ell(0)}(0)e(0). \quad (41)
\end{aligned}$$

In order to minimize the cost of  $\bar{J}_q^*(k)$ ,  $\Upsilon_q(k)$  is taken as  $\Upsilon_q(k) = \check{\Upsilon}_q(k)$ , from which we can obtain

$$K_q(k)\mathcal{C}_q(k) = \Lambda_q^{-1}(k)\bar{Q}_q(k+1)\bar{\mathcal{A}}_q(k) = \mathcal{N}_q(k). \quad (42)$$

According to Lemma 3.1, it is known that  $K_q(k)$  has the form of (34) and, meanwhile, the minimum of the cost function is given by (35). The proof is complete.  $\square$

---

**Algorithm 1 :** Mobile Robot Localization Under SCP.

---

- Step 1:* Set the mobile robot system parameters including the  $H_\infty$  performance index  $\gamma$ , the positive definite matrix  $\mathcal{S}$  and the transition probability matrix  $\Xi(k)$ . Let  $P_q(N) = Q_q(N) = 0$  and  $k = N$ .
- Step 2:* Calculate  $\Delta_q(k)$ ,  $\Lambda_q(k)$ ,  $\mathcal{N}_q(k)$  with known  $P_q(k+1)$  and  $Q_q(k+1)$  via the first equation of (20) and (32) and (33), respectively.
- Step 3:* If  $k \neq 0$ ,  $\Delta_q(k) > 0$  and  $\Lambda_q(k) > 0$ , then derive the filter gain matrix  $K_q(k)$  by (34), obtain  $P_q(k)$  and  $Q_q(k)$  by (19) and the first equation of (31), respectively, set  $k = k - 1$  and go to Step 2; else this algorithm is infeasible, stop.
- Step 4:* Stop.
- 

By means of Theorem 3.3, we give an algorithm for the mobile robot localization with SCP as shown in Algorithm 1.

Until now, the localization algorithm of mobile robot under the SCP has been designed. The advantages of the proposed algorithm can be highlighted as follows: 1) compared with the existing results in [13, 33, 35], a multiple sensor strategy has been applied to the mobile robot localization problem and hence the localization accuracy is expected to be improved; 2) compared with the localization methods of using the multiple sensors in [17, 22, 23], the SCP is, for the first time, introduced in the mobile robot localization problem which effectively handles the issue of data congestion/collision. In the next section, an simulation experiment is implemented to show the effectiveness of the proposed localization algorithm.

#### 4. EXPERIMENTAL RESULTS

In this section, we verify the effectiveness of the proposed localization algorithm on an experimental platform.

Let the sampling period of robot’s odometer, the displacement velocity and the angular velocity be 150ms, 400mm/s and 6rad/s, respectively. The initial states are set as  $x(0) = 0.1\text{m}$ ,  $y(0) = 0.1\text{m}$  and  $\theta(0) = 0.1\text{rad}$ . The positions of landmarks  $M_1$ ,  $M_2$  and  $M_3$  are set as  $(x_{M_1} = 5\text{m}, y_{M_1} = 5\text{m})$ ,  $(x_{M_2} = 7\text{m}, y_{M_2} = 7\text{m})$  and  $(x_{M_3} = 10\text{m}, y_{M_3} = 10\text{m})$ , respectively. The system and measurement noises are chosen as  $\phi(k) = [ 0.2 \sin(0.01k) \quad 0.2 \sin(0.01k) \quad 0.2 \cos(0.01k) ]^T$  and  $v_1(k) = v_2(k) = v_3(k) = [ 0.2 \sin(0.01k) \quad 0.2 \sin(0.01k) ]^T$ . The  $H_\infty$  disturbance attenuation level and the positive definite matrix  $\mathcal{S}$  are chosen as  $\gamma = 3$  and  $\mathcal{S} = \text{diag}\{1, 1, 1, 1, 1, 1, 1, 1\}$ , respectively. The transition probability matrix is taken as  $\Xi(k) = \begin{bmatrix} 0.2 & 0.3 & 0.5 \\ 0.5 & 0.2 & 0.3 \\ 0.3 & 0.5 & 0.2 \end{bmatrix}$ .

The length of the finite horizon is set as  $N = 300$ .

We define the mean errors of the estimates as follows

$$E_x := \frac{1}{N} \sum_{k=1}^N |\hat{x}(k) - \check{x}(k)|, \tag{43}$$

$$E_y := \frac{1}{N} \sum_{k=1}^N |\hat{y}(k) - \check{y}(k)|, \quad (44)$$

$$E_\theta := \frac{1}{N} \sum_{k=1}^N |\hat{\theta}(k) - \check{\theta}(k)|, \quad (45)$$

and the maximum deviations of the estimates as follows

$$M_{ex} := \max_{1 \leq k \leq N} |\hat{x}(k) - \check{x}(k)|, \quad (46)$$

$$M_{ey} := \max_{1 \leq k \leq N} |\hat{y}(k) - \check{y}(k)|, \quad (47)$$

$$M_{e\theta} := \max_{1 \leq k \leq N} |\hat{\theta}(k) - \check{\theta}(k)|. \quad (48)$$

Based on Algorithm 1, the simulation results are shown in Figures 3–6. Figures 3–4 depict the robot position and the angle and their estimates. The position error and the angle error are shown in Figures 5–6, respectively. The mean errors of  $x(k)$ ,  $y(k)$  and  $\theta(k)$  are computed as 0.116m, 0.068m and 0.147rad, respectively and their maximum deviations is obtained as 0.260m, 0.193m and 0.325rad, respectively. The simulation results show that the proposed localization algorithm is effective.

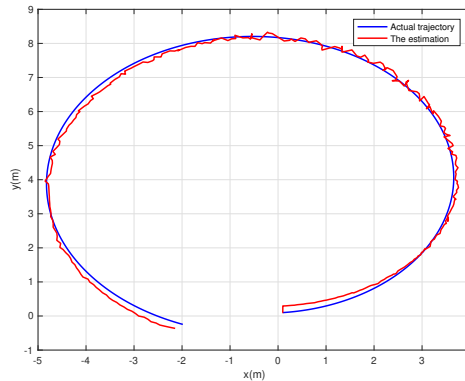


**Fig. 3.** Actual robot trajectory in the  $x - y$  plane and its estimate.

## 5. CONCLUSIONS

In this paper, we have studied the mobile robot localization problem under the SCP. For easing the network burden and reducing network congestion, the SCP has been introduced to govern the transmission of the measurement data. By utilizing the stochastic analysis technique and completing square approach, the filter gain matrices have been

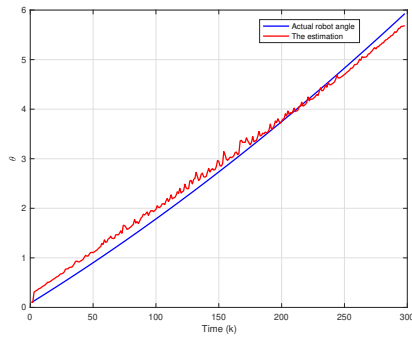


**Fig. 4.** Actual robot angle and its estimate.

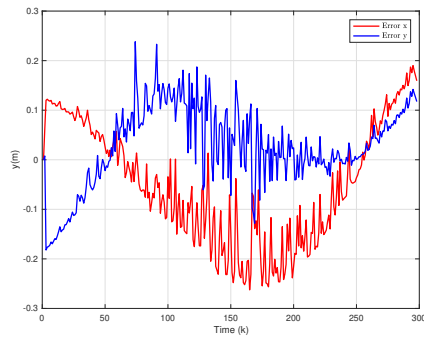


**Fig. 5.** Mobile robot's position error.

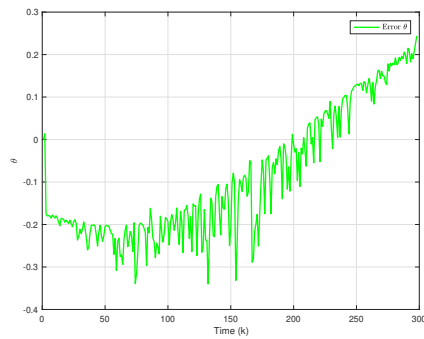


**Fig. 6.** Mobile robot's angle error.

designed by solving two coupled backward recursive RDEs. Based on the proposed filter design scheme, a localization algorithm of mobile robots has been given. Finally, the effectiveness of the proposed localization algorithm has been demonstrated in an experimental platform. Our future research topics would to investigate the localization problem for multiple robots by using the consensus protocol [3, 4, 10, 12, 34, 37, 40] and an energy harvesting sensor based filtering approach [30]. Moreover, our future research topics would also include the extension of the results obtained to the cases of robot systems with cyber-attacks [7, 8, 14] and stochastic noises [27, 28].

#### ACKNOWLEDGEMENT

This work was partially supported by the National Natural Science Foundation of China under Grants 61873059, the Program for Professor of Special Appointment (Eastern Scholar) at Shanghai Institutions of Higher Learning of China, the Natural Science Foundation of Shanghai under Grant 18ZR1401500, and the Fundamental Research Funds for the Central Universities and Graduate Student Innovation Fund of Donghua University under Grant CUSF-DH-D-2019087.

(Received October 15, 2019)

#### REFERENCES

---

- [1] J. Chen and H. Qiao: Muscle-synergies-based neuromuscular control for motion learning and generalization of a musculoskeletal system. *IEEE Trans. Systems Man Cybernet.: Systems* (2020), 1–14.
- [2] S. Y. Chen: Kalman filter for robot vision: A survey. *IEEE Trans. Industr. Electron.* *59* (2012), 11, 4409–4420. DOI:10.1109/tie.2011.2162714
- [3] W. Chen, D. Ding, X. Ge, Q. Han, and G. Wei:  $H_\infty$  containment control of multiagent systems under event-triggered communication scheduling: The finite-horizon case. *IEEE Trans. Cybernet.* *50* (2020), 4, 1372–1382. DOI:10.1109/tcyb.2018.2885567
- [4] D. Ding, Q. Han, Z. Wang, and X. Ge: A survey on model-based distributed control and filtering for industrial cyber-physical systems. *IEEE Trans. Industr. Inform.* *15* (2019), 5, 2483–2499. DOI:10.1109/tii.2019.2905295
- [5] D. Ding, Z. Wang, and Q. Han: Neural-network-based output-feedback control with stochastic communication protocols. *Automatica* *106* (2019), 221–229. DOI:10.1016/j.automatica.2019.04.025
- [6] D. Ding, Z. Wang, Q. Han, and G. Wei: Neural-network-based output-feedback control under round-robin scheduling protocols. *IEEE Trans. Cybernet.* *49* (2019), 6, 2372–2384. DOI:10.1109/tcyb.2018.2827037
- [7] D. Ding, Z. Wang, Q. Han, and G. Wei: Security control for discrete-time stochastic nonlinear systems subject to deception attacks. *IEEE Trans. Systems Man Cybernet.: Systems* *48* (2018), 5, 779–789. DOI:10.1109/tsmc.2016.2616544
- [8] D. Ding, Z. Wang, D. W. C. Ho, and G. Wei: Distributed recursive filtering for stochastic systems under uniform quantizations and deception attacks through sensor networks. *Automatica* *78* (2017), 231–240. DOI:10.1016/j.automatica.2016.12.026



- [9] H. Dong, N. Hou, Z. Wang, and H. Liu: Finite-horizon fault estimation under imperfect measurements and stochastic communication protocol: Dealing with finite-time boundedness. *Int. J. Robust Nonlinear Control* *29* (2019), 1, 117–134. DOI:10.1002/rnc.4382
- [10] X. Ge and Q. Han: Consensus of multiagent systems subject to partially accessible and overlapping Markovian network topologies. *IEEE Trans. Cybernet.* *47* (2017), 8, 1807–1819. DOI:10.1109/tcyb.2016.2570860
- [11] X. Ge, Q. Han, and Z. Wang: A dynamic event-triggered transmission scheme for distributed set-membership estimation over wireless sensor networks. *IEEE Trans. Cybernet.* *49*(2019), 1, 171–183. DOI:10.1109/tcyb.2016.2570860
- [12] X. Ge, Q. Han, and Z. Wang: A threshold-parameter-dependent approach to designing distributed event-triggered  $H_\infty$  consensus filters over sensor networks. *IEEE Trans. Cybernet.* *49* (2019), 4, 1148–1159. DOI:10.1109/tcyb.2017.2789296
- [13] R. P. Guan, B. Ristic, L. Wang, B. Moran, and R. Evans: Feature-based robot navigation using a Doppler-azimuth radar. *Int. J. Control* *90* (2017), 4, 888–900. DOI:10.1080/00207179.2016.1244727
- [14] L. Hu, Z. Wang, Q. Han, and X. Liu: State estimation under false data injection attacks: Security analysis and system protection. *Automatica* *87* (2018), 176–183. DOI:10.1016/j.automatica.2017.09.028
- [15] C. Huang, B. Shen, H. Chen, and H. Shu: A dynamically event-triggered approach to recursive filtering with censored measurements and parameter uncertainties. *J. Franklin Inst.* *356* (2019), 15, 8870–8889. DOI:10.1016/j.jfranklin.2019.08.029
- [16] A. Khan, B. Rinner, and A. Cavallaro: Cooperative robots to observe moving targets: Review. *IEEE Trans. Cybernet.* *48* (2018), 1, 187–198. DOI:10.1109/tcyb.2016.2628161
- [17] Y. Kim, J. An, and J. Lee: Robust navigational system for a transporter using GPS/INS fusion. *IEEE Trans. Industr. Electron.* *65* (2018), 4, 3346–3354. DOI:10.1109/tie.2017.2752137
- [18] S. Leutenegger, S. Lynen, M. Bosse, R. Siegwart, and P. Furgale: Keyframe-based visual-inertial odometry using nonlinear optimization. *Int. J. Robotics Res.* *34* (2015), 3, 314–334. DOI:10.1177/0278364914554813
- [19] B. Li, Z. Wang, Q. Han, and H. Liu: Input-to-state stabilization in probability for nonlinear stochastic systems under quantization effects and communication protocols. *IEEE Trans. Cybernet.* *49* (2019), 9, 3242–3254. DOI:10.1109/tcyb.2018.2839360
- [20] Q. Li, B. Shen, Z. Wang, T. Huang, and J. Luo: Synchronization control for a class of discrete time-delay complex dynamical networks: A dynamic event-triggered approach. *IEEE Trans. Cybernet.* *49* (2019), 5, 1979–1986. DOI:10.1109/tcyb.2018.2818941
- [21] R. Li and H. Qiao: A survey of methods and strategies for high-precision robotic grasping and assembly tasks-some new trends. *IEEE/ASME Trans. Mechatronics* *24* (2019), 6, 2718–2732. DOI:10.1109/tmech.2019.2945135
- [22] X. Li, W. Chen, C. Chan, B. Li, and X. Song: Multi-sensor fusion methodology for enhanced land vehicle positioning. *Inform. Fusion* *46* (2019), 51–62. DOI:10.1016/j.inffus.2018.04.006
- [23] H. Liu, F. Sun, B. Fang, and X. Zhang: Robotic room-level localization using multiple sets of sonar measurements. *IEEE Trans. Instrument. Measurement* *66* (2017), 1, 2–13. DOI:10.1109/tim.2016.2618978

- [24] S. Lowry, N. Sunderhauf, P. Newman, J. J. Leonard, D. Cox, P. Corke, and M. J. Milford: Visual place recognition: A survey. *IEEE Trans. Robotics* *32* (2016), 1, 1–19. DOI:10.1109/tro.2015.2496823
- [25] R. C. Luo and T. J. Hsiao: Dynamic wireless indoor localization incorporating with an autonomous mobile robot based on an adaptive signal model fingerprinting approach. *IEEE Trans. Industr. Electron.* *66* (2019), 3, 1940–1951. DOI:10.1109/tie.2018.2833021
- [26] Y. Luo, Z. Wang, G. Wei, F. E. Alsaadi, and T. Hayat: State estimation for a class of artificial neural networks with stochastically corrupted measurements under round-robin protocol. *Neural Networks* *77* (2016), 70–79. DOI:10.1016/j.neunet.2016.01.001
- [27] L. Ma, Z. Wang, Y. Liu, and F. E. Alsaadi: Distributed filtering for nonlinear time-delay systems over sensor networks subject to multiplicative link noises and switching topology. *Int. J. Robust Nonlinear Control* *29* (2019), 10, 2941–2959. DOI:10.1002/rnc.4535
- [28] L. Ma, Z. Wang, Q. Han, and Y. Liu: Dissipative control for nonlinear Markovian jump systems with actuator failures and mixed time-delays. *Automatica* *98* (2018), 358–362. DOI:10.1016/j.automatica.2018.09.028
- [29] B. Shen, Z. Wang, and H. Qiao: Event-triggered state estimation for discrete-time multidelayed neural networks with stochastic parameters and incomplete measurements. *IEEE Trans. Neural Networks Learning Systems* *28* (2017), 5, 1152–1163. DOI:10.1109/tnnls.2016.2516030
- [30] B. Shen, Z. Wang, D. Wang, J. Luo, H. Pu, and Y. Peng: Finite-horizon filtering for a class of nonlinear time-delayed systems with an energy harvesting sensor. *Automatica* *100* (2019), 144–152. DOI:10.1016/j.automatica.2018.11.010
- [31] X. Wan, Z. Wang, Q. Han, and M. Wu: A recursive approach to quantized  $H_\infty$  state estimation for genetic regulatory networks under stochastic communication protocols. *IEEE Trans. Neural Networks Learning Systems* *30* (2019), 9, 2840–2852. DOI:10.1109/tnnls.2018.2885723
- [32] X. Wan, Z. Wang, Q. Han, and M. Wu: Finite-time  $H_\infty$  state estimation for discrete time-delayed genetic regulatory networks under stochastic communication protocols. *IEEE Trans. Circuits Systems I: Regular Papers* *65* (2018), 10, 3481–3491. DOI:10.1109/tcsi.2018.2815269
- [33] Z. Wang, H. Dong, B. Shen, and H. Gao: Finite-horizon  $H_\infty$  filtering with missing measurements and quantization effects. *IEEE Trans. Automat. Control* *58* (2013), 7, 1707–1718. DOI:10.1109/tac.2013.2241492
- [34] W. Xu, D. W. C. Ho, L. Li, and J. Cao: Event-triggered schemes on leader-following consensus of general linear multiagent systems under different topologies. *IEEE Trans. Cybernetics* *47* (2017), 1, 212–223. DOI:10.1109/tcyb.2015.2510746
- [35] F. Yang, Z. Wang, S. Lauria, and X. Liu: Mobile robot localization using robust extended  $H_\infty$  filtering. *Proc. Inst. Mechanical Engineers, Part I: J. Systems Control Engrg.* *223* (2009), 8, 1067–1080. DOI:10.1243/09596518jsce791
- [36] X. Zhang and Q. Han: A decentralized event-triggered dissipative control scheme for systems with multiple sensors to sample the system outputs. *IEEE Trans. Cybernet.* *46* (2016), 12, 2745–2757. DOI:10.1109/tcyb.2015.2487420
- [37] X. Zhang, Q. Han, X. Ge, D. Ding, L. Ding, D. Yue, and C. Peng: Networked control systems: A survey of trends and techniques. *IEEE/CAA J. Automat. Sinica* (2019), 1–17. DOI:10.1109/tcyb.2015.2487420

- [38] L. Zou, Z. Wang, and H. Gao: Observer-based  $H_\infty$  control of networked systems with stochastic communication protocol: The finite-horizon case. *Automatica* 63 (2016), 366–373.
- [39] L. Zou, Z. Wang, and H. Gao: Set-membership filtering for time-varying systems with mixed time-delays under round-robin and weighted try-once-discard protocols. *Automatica* 74 (2016), 341–348. DOI:10.1016/j.automatica.2016.07.025
- [40] Z. Zuo, Q. Han, B. Ning, X. Ge, and X. Zhang: An overview of recent advances in fixed-time cooperative control of multiagent systems. *IEEE Trans. Industr. Inform.* 14 (2018), 6, 2322–2334. DOI:10.1109/tii.2018.2817248

*Yanyang Lu, Corresponding author. 1. College of Information Science and Technology, Donghua University, Shanghai 201620, P. R. China; 2. Engineering Research Center of Digitalized Textile and Fashion Technology, Ministry of Education, Shanghai 201620. P. R. China.*

*e-mail: yanyang.lu@mail.dhu.edu.cn*

*Bo Shen, 1. College of Information Science and Technology, Donghua University, Shanghai 201620, P. R. China; 2. Engineering Research Center of Digitalized Textile and Fashion Technology, Ministry of Education, Shanghai 201620. P. R. China.*

*e-mail: bo.shen@dhu.edu.cn*